

A LABORATORY INVESTIGATION OF THE RELATIVE DISSOLUTION RATES OF THE LIRIO LIMESTONE AND THE ISLA DE MONA DOLOMITE AND IMPLICATIONS FOR CAVE AND KARST DEVELOPMENT ON ISLA DE MONA

MYRNA IRIS MARTINEZ¹ AND WILLIAM B. WHITE²

Department of Geosciences, The Pennsylvania State University, University Park, PA 16802 USA

The relative dissolution kinetics of the Lirio Limestone and the Isla de Mona Dolomite were determined by dissolving discs of various samples in CO₂-saturated solutions. Rate curves for carbonate dissolution were determined by monitoring pH and specific conductance as a function of time. Dissolution rates for limestone samples were distinctly higher than rates for dolomite samples but the rate curves had similar shapes. Initial rates for limestones averaged 12.53 $\mu\text{mol m}^{-2} \text{sec}^{-1}$ compared with 8.53 for dolomite. The limestone rates are comparable with those measured on single crystal calcite but the dolomite rates are higher than rates measured on Paleozoic dolomites. The relative dissolution rates are sufficient to be a factor in explaining the concentration of caves at the limestone/dolomite contact but may not be the only controlling factor.

Isla de Mona is a 6-km wide carbonate island located in the deep water of the Mona Passage about halfway between Puerto Rico and the Dominican Republic. Except for small beach areas on the south side, the island is bounded by cliffs rising up to 90 m msl. The main portion of the island is a karst plateau underlain by the Miocene Lirio Limestone. The core of the island is composed of the Isla de Mona Dolomite (Kaye 1959; Frank *et al.* 1998a). There are many caves on the island, mostly located on the plateau escarpment near the contact between the limestone and the dolomite (Frank 1993; Frank *et al.* 1998b).

There is a marked contrast in the response to dissolution of the Lirio Limestone and the Isla de Mona Dolomite. The Lirio Limestone comprises most of the plateau surface and is breached to expose the underlying dolomite only at the large closed depression of Bajura de los Cerezos (Briggs & Seiders 1972). Elsewhere, the Isla de Mona Dolomite is exposed at the surface only on the sea cliffs. The Lirio Limestone is sculptured into a complex karren surface on much of the plateau and is penetrated by many shafts. As far as has been observed the shafts splay out into short horizontal dissolution openings at the limestone/dolomite contact. They do not penetrate significantly into the dolomite (Frank 1993). Likewise, cave development is largely limited to the basal Lirio Limestone. Accepting the hypothesis that the large caves on Isla de Mona are mixing zone caves (Frank *et al.* 1998b), there remains the problem of why there are so few caves in the dolomite. Interpretation of the groundwater flow system on Isla de Mona

depends strongly on whether or not conduits occur deep within the dolomite, perhaps as drains to the coast during low stands of sea level. So far, evidence for any type of conduit permeability at or below the present water table is sparse. Only Cueva del Agua de Puente Brava, at the base of the sea cliff, reaches to the water table.

In the Paleozoic carbonate rocks of the Appalachians, dolomites tend to exhibit substantially less karst development than do limestones (Rauch & White 1970). Limestone surfaces may exhibit deep closed depressions while nearby dolomite terrain exhibits only shallow swales. Large caves and integrated drainage systems develop in the limestones; caves range from small to nonexistent in the dolomites. This contrast arises from the substantially different rates of dissolution of calcite and dolomite, and one must entertain the hypothesis that similar lithologic controls may operate on Isla de Mona. It must be demonstrated, however, that the Miocene carbonate rocks of Isla de Mona with their high primary permeability do, in fact, function in a geochemically similar way to the dense, low permeability Paleozoic carbonates of eastern United States.

The objective of this investigation was to compare the dissolution kinetics of the Lirio Limestone and the Isla de Mona Dolomite by means of a quantitative laboratory investigation. The rates of dissolution of selected samples of Lirio Limestone and Isla de Mona Dolomite were measured in CO₂-saturated water. These results then can be compared with other investigations of calcite and dolomite dissolution.

¹ Present address: 100 Carmen Hills Drive, Box 141, San Juan, Puerto Rico 00926; myrna_iris@yahoo.com

² Also affiliated with The Materials Research Laboratory.

SAMPLE SELECTION AND CHARACTERIZATION

Kilogram size samples of both rock formations were collected at several locations on the island. The mineral compositions of these samples were determined by X-ray powder diffraction. Sample locations and mineral identifications are given in Table 1.

Acetate peels were prepared in duplicate for each sample. One of each of the duplicates was stained using a combination of Alizarin Red-S and potassium ferricyanide stains. Pink to red color indicates calcite, mauve to blue indicates ferroan calcite, no color indicates dolomite, and a very pale blue indicates ferroan dolomite. All peels were studied with a petrographic microscope.

LLC: The rock is white, with a fine-grained matrix, and is composed of at least 50% allochems. All allochems are fossils, mainly corals. Well preserved gastropods can be seen. Most of the rock stained a deep pink color in confirmation of the x-ray results.

LLL: The rock is very dense, fine-grained limestone with low porosity. The color is white to beige. The only fossils that can be easily recognized are corals, some of which are crystalline, an indication of calcite replacement. The rock stained from light to dark pink.

LLVC: The rock shows strong evidence of dolomitization. Although the geologic map shows the collection area as limestone, the collection point at the bottom of a 10-m pit is apparently in a transition zone between limestone and dolomite. The x-ray pattern indicates somewhat less than half of the sample is calcite while the remainder is dolomite. The more continuous matrix did not stain. About 50-70% of the observable crystals were very well defined dolomite rhombs.

MDB: The rock was cream to bone white. The matrix was fine-grained, fairly massive with a large vuggy porosity. Small fossils are abundant, particularly bivalve shells and pieces of coral. The larger fossils have been dissolved and have been replaced by crystals visible with a hand lens. The bulk rock was unstained in agreement with x-ray results indicating that most of the rock was dolomite. Some of the larger grains stained pink. Most of the fossils were only partially stained, indicating only partial replacement of the original shell material. Some vuggy porosity can still be seen under the microscope and some calcite cement is still present.

MDL: The rock is very fine-grained with a sugary texture. It has some vuggy and moldic porosity. Most of the recognizable fossils are corals. The rock picked up a very light pink stain and there are some patches of calcite scattered in the matrix. The calcite was not detected by x-ray which showed only a well-crystallized and well-ordered dolomite.

Although dissolution experiments were performed on all five rock samples, LLC and LLL were taken as monomineralic limestones while MDL was the closest to a monomineralic dolomite so that these specimens should give the strongest contrast in dissolution kinetics.

Table 1. Location and Description of Rock Specimens

Code	Rock Type	Location	Mineralogy*
LLC	Lirio Limestone	Plateau surface near Cueva El Capitan	Calcite
LLL	Lirio Limestone	Cliff face below Cueva del Lirio	Calcite
LLVC	Lirio Limestone	Bottom of pit, along trail to Bajura de los Cerezos. 10 m below surface, near Lirio/Mona contact.	40% calcite
MDB	Mona Dolomite	Northwest corner of island between Punte Capitan and Cabo Noroeste.	60% dolomite 90% dolomite 10% calcite
MDL	Mona Dolomite	At sea level below Cueva del Lirio	Dolomite

*Mineral percentages determined from relative intensities of X-ray diffraction lines.

EXPERIMENTAL METHODS

The experimental procedure followed those developed earlier in this laboratory by Herman (1982; Herman & White 1985). The rock specimens were sawed into slabs about 12 mm thick. Circular disks about 40 mm in diameter were cut from the slabs with a diamond core drill. These were mounted in a chuck and sealed so that only one face of the disk was exposed to the solution. The effective diameter of each disk was measured with calipers. The apparatus for the dissolution experiments is sketched in figure 1. It consists of a vessel containing 800 mL of solution held in a constant temperature bath at 25°C. The sample in its chuck was attached by a drive shaft to a gear box that allowed the sample disk to be spun at various angular velocities. Also inserted into the solution was a conductivity probe and a pH electrode. The solution was continuously saturated with CO₂ bubbled from a tank through a fritted glass disperser.

The spinning disk technique allows dissolution to take place with constant mass transfer across the surface of the disk (Levich 1962). For these experiments a single rotation rate of 225 rpm was chosen. This corresponds to a Reynolds number of 11,200 at 25°C.

Both pH and specific conductance measurements were recorded at specific time intervals. Data were recorded every hour in the early stages of a dissolution run and every few hours as the experiment progressed. Total run times were about five days. All runs were made in duplicate. Samples of 1.0 mL or less were drawn eight times in the course of each run and analyzed for Ca and Mg by atomic emission spectroscopy. These analyses allowed the determination of the relation between specific conductance and hardness specifically calibrated for the Isla de Mona rocks.

RESULTS

BACKGROUND CHEMISTRY AND DATA PROCESSING

The gas bubbled through the solution was pure CO₂ saturated with water vapor. Because the solution was kept constantly saturated with CO₂, it behaves as an open system with a constant P_{CO₂}. Taking account of the elevation of the laboratory (350 m) and deducting the contribution from the vapor

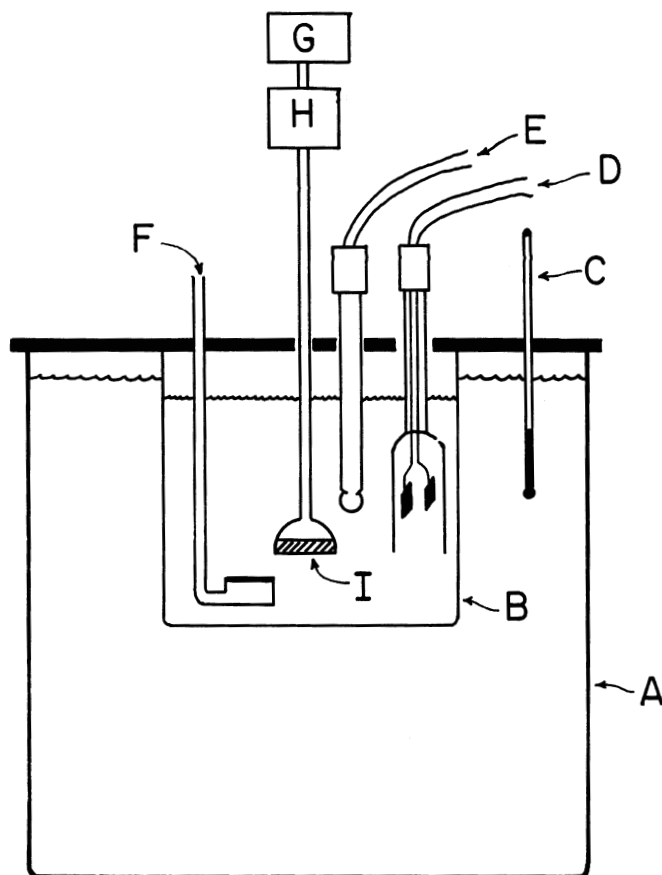


Figure 1. Schematic drawing of experimental apparatus. A = constant temperature bath set at 25°C. B = beaker containing 800 mL of aqueous solution. C = thermometer. D = Conductivity electrode. E = pH electrode. F = CO₂ inlet through fitted glass disk. G = drive motor. H = gear reduction box. I = disk of experimental sample.

pressure of water, $P_{\text{CO}_2} = 0.93$ atm for all experiments.

By assuming equilibrium among the dissolved CO₂, H₂CO₃^o, and HCO₃⁻, before the disk was inserted, the initial pH was calculated to be 3.93, in good agreement with the measured value. If the dissolution reaction was assumed to go to equilibrium, the final pH was calculated, using equations derived by Drever (1997), to be 5.93.

Dissolved Ca + Mg concentrations in units of millimoles/liter, as determined by chemical analysis, were plotted against the corresponding values for specific conductance, Spc (Fig. 2). There is a surprising amount of scatter. Hardness/conductance plots of spring waters typically exhibit varying degrees of scatter because of variations in other constituents of the water. Laboratory investigations usually produce very tight fits of the data. The source of the scatter is not known but the scatter reduces the precision with which Ca + Mg can be measured. Fitting a linear regression to the data in figure 2 gives the result:

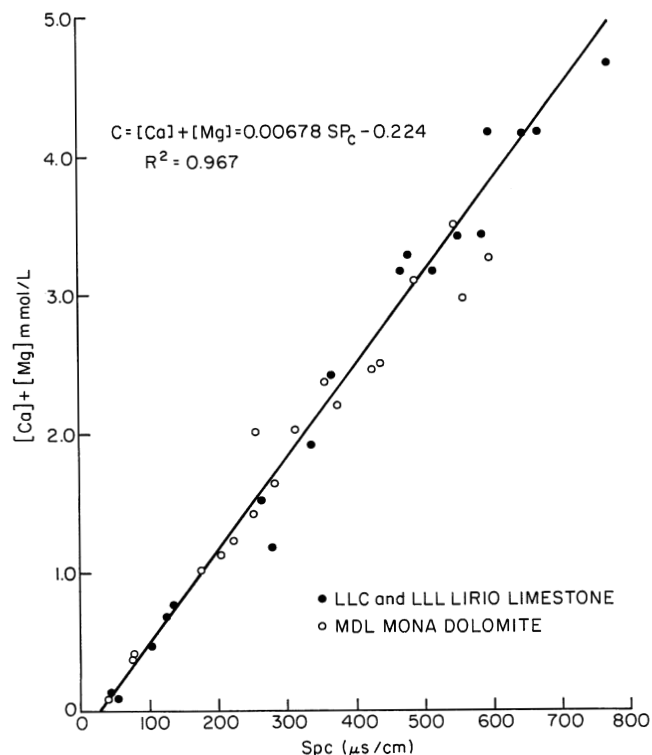


Figure 2. Relation of [Ca] + [Mg] determined by atomic emission spectroscopy to specific conductance for limestone and dolomite samples. Solid line represents the linear regression of all data points.

$$[\text{Ca}] + [\text{Mg}] = 0.00678\text{Spc} - 0.244 \quad [1]$$

where concentrations are given in millimoles/liter. Limestone and dolomite data are very similar so that a single regression was fitted to both data sets. Equation [1] was used to extract [Ca] + [Mg] from specific conductance data collected during the kinetics experiments.

The overall reactions for dissolution of calcite and dolomite are:



Charge neutrality requires that:

$$[\text{H}^+] + 2[\text{Ca}^{2+}] = [\text{HCO}_3^-] \quad [2]$$

which in terms of activities is:

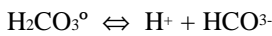
$$\frac{a_{\text{H}^+}}{\gamma_{\text{H}^+}} + 2 \frac{a_{\text{Ca}^{2+}}}{\gamma_{\text{Ca}^{2+}}} = \frac{a_{\text{HCO}_3^-}}{\gamma_{\text{HCO}_3^-}} \quad [3]$$

where a is activity of the given ion and γ is the activity coefficient.

If the reactions:



$$\frac{a_{\text{H}_2\text{CO}_3}}{P_{\text{CO}_2}} = K_{\text{CO}_2} \quad [4]$$



$$\frac{a_{\text{H}^+} a_{\text{HCO}_3^-}}{a_{\text{H}_2\text{CO}_3}} = K_1 \quad [5]$$

are assumed to be in equilibrium (a good assumption on the time scale of these experiments), the bicarbonate activity for a system open to CO_2 is given by:

$$a_{\text{HCO}_3^-} = \frac{K_1 K_{\text{CO}_2} P_{\text{CO}_2}}{a_{\text{H}^+}} \quad [6]$$

where the K s are the equilibrium constants for the given reactions.

Substituting equation [6] into equation [3] and rearranging terms provides the needed relationship for calculation of $[\text{Ca}^{2+}]$ from measured pH.

$$[\text{Ca}^{2+}] = \frac{1}{2} \left[\frac{K_1 K_{\text{CO}_2} P_{\text{CO}_2}}{\gamma_{\text{HCO}_3^-} a_{\text{H}^+}} - \frac{a_{\text{H}^+}}{\gamma_{\text{H}^+}} \right] \quad [7]$$

The equation for dolomite is the same except that the calculation gives $[\text{Ca}] + [\text{Mg}]$.

Equation [7] was used to extract the amount of dissolved $\text{Ca} + \text{Mg}$ from the measured pH. The concentrations of $[\text{Ca}] + [\text{Mg}]$ calculated from specific conductance were used to estimate ionic strength and thus to calculate the activity coefficient for the bicarbonate ion.

LIMESTONE AND DOLOMITE DISSOLUTION

Full rate curves for three pairs of samples, two limestones and one dolomite are shown in figure 3. These samples were selected because LLC and LLL were phase-pure calcite and MDL was close to a phase-pure dolomite. The reproducibility between runs is 10-20% but the scatter of individual data points is much smaller indicating that the mismatch between duplicate pairs is due to the heterogeneities of the rock samples themselves rather than error in the measurements. Sample LLC, in particular is a highly porous and vuggy limestone so that the effective surface area is much larger than the geometric area of the disk.

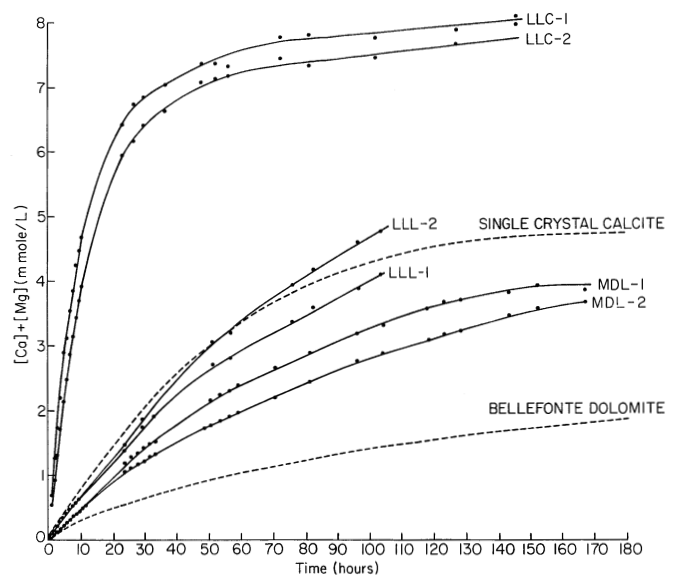


Figure 3. Dissolution rate curves for duplicate runs of samples LLC, LLL, and MDL. $[\text{Ca}] + [\text{Mg}]$ of limestone samples determined from pH; $[\text{Ca}] + [\text{Mg}]$ of dolomite sample determined from specific conductance. Single crystal calcite data (dashed curves) from Herman (1982).

The saturation concentration of $[\text{Ca}^{2+}]$ based on pure calcite at $P_{\text{CO}_2} = 0.93$ atm is calculated to be 8.145 mmol/L. Only sample LLC approaches saturation on the time scale of the experiments. The more massive limestone, LLL, dissolved rapidly but had reached only about half saturation at the termination of the experiment. The dolomite runs were continued longer but dolomite MDL had not approached equilibrium after 7 days.

INITIAL RATES

To compare the dissolution rates of one rock type with another, it is convenient to examine the initial rate when the solutions are far from equilibrium. The rate curves are essentially linear over the first 10 hours of the experiments (Fig. 4) so that the initial rate can be described by:

$$\text{Rate} = \frac{V}{A} \frac{dC}{dt} \quad [8]$$

where V = volume of solution (800 mL in all experiments), A = area of exposed face of disk, and dC/dt is the slope of the near-linear plot of concentration against time. The data for each experimental run were fitted by linear regression of the data to obtain dC/dt for each experiment. The experimental data were collected with $[\text{Ca}] + [\text{Mg}]$ in units of mmol/L and time in hours. These units were converted to calculate the initial rates in units of $\mu\text{mol m}^{-2} \text{sec}^{-1}$ (Table 2). The lines in figure 4 are linear regressions using data for duplicate runs of each of the rock samples.

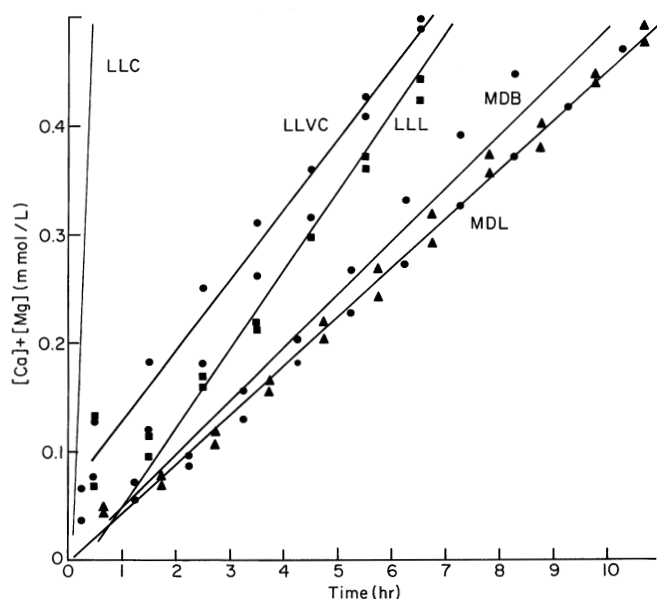


Figure 4. Initial dissolution rates for all samples. Solid lines represent linear regressions through both duplicate run data sets for each sample. Data points for LLC fall off the scale on this plot.

Table 2. Initial Dissolution Rates.

Sample Code	A (cm ²)	dC/dt (mol/L-hr)	Rate ($\mu\text{mol m}^{-2} \text{sec}^{-1}$)
LLC-1	12.24	0.420	76.24
LLC-2	12.13	0.361	66.13
LLL-1	12.55	0.0766	13.56
LLL-2	12.45	0.0704	12.57
LLVC-1	12.19	0.0703	12.81
LLVC-2	12.19	0.0610	11.12
MDB-1	12.25	0.0551	9.99
MDB-2	12.16	0.0435	7.95
DMDB-1	12.25	0.0450	8.16
DMDB-2	12.16	0.0473	8.64
MDL-1	12.18	0.0450	8.21
MDL-2	12.34	0.0457	8.23
Calcite*	12.74	-----	11.66
Dolomite*	13.33	-----	4.11

*Single crystal calcite and Bellefonte (Ordovician) dolomite from data of Herman (1982).

CALCIUM/MAGNESIUM RATIOS

Dissolution of the dolomite sample MDL gives values of $[\text{Ca}]/[\text{Mg}]$ of 1.61 for the first run and 1.47 for the second run. These ratios do not change as the experiment progresses. The solutions are somewhat more calcium-rich than expected for a stoichiometric dolomite but consistent with the petrologic examination which suggests some calcite in the dolomite. In contrast, the $[\text{Ca}]/[\text{Mg}]$ ratio changes continuously as the limestone specimens were dissolved (Fig. 5). Both runs on specimen LLL are plotted. The concentration of magnesium in solution is in the range of 0.5 to 1.5 mg/L, resulting in large analytical uncertainties and corresponding scatter in the ratios. The Ca^{2+} ion concentration increases as the dissolution reac-

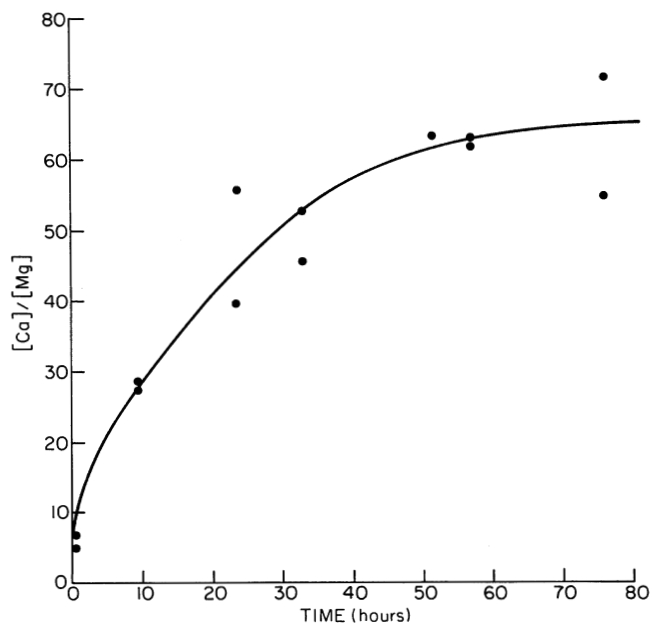


Figure 5. Change with time of $[\text{Ca}]/[\text{Mg}]$ for limestone sample LLL.

tion proceeds whereas the Mg^{2+} ion concentration increases only slightly.

COMPARISON WITH LITERATURE DATA

A direct comparison can be made with the single crystal results of Herman (1982) because her study also used the spinning disk technique with nearly the same area disks. Herman found that dissolution rates under highly undersaturated conditions were strongly dependent on Reynolds number. Two of Herman's rate curves, one for single crystal calcite and one for the dense Ordovician Bellefonte Dolomite are drawn on figure 3. The agreement is excellent between the rate of dissolution of the Lirio Limestone (Sample LLL) and the single crystal calcite. In contrast, the rate of dissolution of the Isla de Mona Dolomite is about twice the rate of dissolution of the Bellefonte Dolomite. Mineralogic and lithologic examination of the Isla de Mona Dolomite reveals a substantial quantity of calcite interspersed with a well-ordered dolomite. It seems likely that the calcite is responsible for the high dissolution rate compared to the dense Paleozoic dolomite.

A set of experiments on the dissolution rate of Paleozoic limestones (Rauch & White 1977) used a different geometry. Solutions were pumped through holes drilled into limestone blocks. In spite of the difference in geometry, the results are similar to those obtained using the spinning disk technique.

Recent experimental results (Dreybrodt *et al.* 1996; Liu & Dreybrodt 1997) show that there are three rate-determining processes: reaction rate controlled kinetics at the mineral/water interface, mass transport by diffusion, and the slow kinetics of the hydration of dissolved carbon dioxide. As a result, the results of laboratory experiments conducted at high carbon

dioxide pressures must be applied with caution to natural systems where carbon dioxide pressures are usually much lower.

APPLICATION TO CAVE AND KARST DEVELOPMENT ON ISLA DE MONA

In broad terms, the caves of Isla de Mona fall into two categories: the large mixing-zone caves near the coast and shafts with minor caves scattered over the Plateau. The mixing zone caves and the splay passages at the bases of the shafts occur mainly at the contact between the limestone and dolomite. We can now turn to the question that this experimental investigation was intended to address. Can one account for the general absence of cave development in the dolomite solely in terms of a slower dissolution rate for the dolomite? The answer is that it is probably only part of the reason. The dolomite definitely dissolves more slowly than the limestone and this is part of the reason that cave development fades out at the contact. But the dissolution rate contrast is not as great as the rate contrast between Paleozoic limestones and dolomites.

There are no geochemical data on the infiltration waters on Isla de Mona. The soils on the Plateau are either thin or non-existent. Rainfall on the Plateau has little opportunity to pick up CO₂ much beyond the atmospheric background. The aggressivity of the water, low to begin with, is quickly lost in the dissolution of the limestone surface in the Lirio Limestone. Water reaching the underlying dolomite would have a low CO₂ partial pressure and not be highly undersaturated. This factor would also contribute to the absence of conduit dissolution in the dolomite. Our proposed interpretation, based in part only on geologic evidence, is that it is a combination of slower kinetics and the CO₂-poor infiltration water that restricts cave development to the Lirio Limestone and the Lirio/Isla de Mona contact zone. In the absence of additional geochemical data, more precise interpretation is difficult.

CONCLUSIONS

Dissolution rates were measured on samples of Lirio Limestone and Isla de Mona Dolomite under experimental conditions of 25°C, P_{CO₂} = 0.93 atm, and Reynolds number = 11,200. Bulk limestone dissolved at about the same rate as single crystal calcite. The high porosity and thus high surface area of some limestones creates greatly enhanced apparent dissolution rates. The dissolution rate of the Mona Dolomite was about half the dissolution rate of the limestone but about twice the dissolution rate of dense Paleozoic dolomite.

It was concluded that differences in dissolution rate alone were only one factor in accounting for the absence of conduit development in the dolomite. It seems likely that CO₂ content and degree of saturation of infiltrating storm water also play an important role.

ACKNOWLEDGEMENTS

This investigation was an outgrowth of the Isla de Mona Project, directed by Joseph W. Troester and Carol M. Wicks. We are grateful to the U.S. Geological Survey, Water Resources Division, and to the Puerto Rico Departamento de Recursos Naturales for their support of the field work of this investigation.

REFERENCES

- Briggs, R.P. & Seiders, V.M. (1972). Geologic map of the Isla de Mona Quadrangle, Puerto Rico. U.S. Geological Survey Miscellaneous Geologic Map Investigations Map 1-718, 1 sheet with text.
- Drever, J.I. (1997). *The Geochemistry of Natural Waters*. 3rd Edition. Prentice Hall, Upper Saddle River, NJ: 436 pp.
- Dreybrodt, W., Lauckner, J., Liu, Z., Svensson, U., & Buhmann, D. (1996). The kinetics of the reaction CO₂ + H₂O ⇌ H⁺ + HCO₃⁻ as one of the rate limiting steps for the dissolution of calcite in the system H₂O-CO₂-CaCO₃. *Geochimica et Cosmochimica Acta* 60: 3375-3381.
- Frank, E.F. (1993). *Aspects of karst development and speleogenesis, Isla de Mona, Puerto Rico: An analogue for Pleistocene speleogenesis in the Bahamas*. M.S. thesis, Geology, Mississippi State University: 132 pp.
- Frank, E.F., Wicks, C., Mylroie, J., Troester, J., Alexander, E.C., Jr., & Carew, J.L. (1998a). Geology of Isla de Mona, Puerto Rico. *Journal of Cave and Karst Studies* 60(2): 69-72.
- Frank, E.F., Mylroie, J., Troester, J., Alexander, E.C., Jr., & Carew, J.L. (1998b). Karst development and speleogenesis, Isla de Mona, Puerto Rico. *Journal of Cave and Karst Studies* 60(2): 73-83.
- Herman, J.S. (1982). *The dissolution kinetics of calcite, dolomite, and dolomitic rocks in the CO₂-water system*. Ph.D. thesis, Geochemistry and Mineralogy, The Pennsylvania State University: 214 pp.
- Herman, J.S. & White, W.B. (1985). Dissolution kinetics of dolomite: Effects of lithology and fluid flow velocity. *Geochimica et Cosmochimica Acta* 49: 2017-2026.
- Kaye, C.A. (1959). Geology of Isla Mona, Puerto Rico, and notes on the age of Mona Passage. *U.S. Geological Survey Professional Paper* 317-C: 141-178.
- Levich, V.G. (1962). *Physicochemical Hydrodynamics*. Prentice Hall, Englewood Cliffs, NJ: 700 pp.
- Liu, Zaihua & Dreybrodt, W. (1997). Dissolution kinetics of calcium carbonate minerals in H₂O-CO₂ solutions in turbulent flow: The role of the diffusion boundary layer and the slow reaction H₂O + CO₂ ⇌ H⁺ + HCO₃⁻. *Geochimica et Cosmochimica Acta* 61: 2879-2889.
- Rauch, H.W. & White, W.B. (1970). Lithologic controls on the development of solution porosity in carbonate aquifers. *Water Resources Research* 6: 1175-1192.
- Rauch, H.W. & White, W.B. (1977). Dissolution kinetics of carbonate rocks. 1. Effects of lithology on dissolution rate. *Water Resources Research* 13: 381-394.